Mechanics of Column Beds: I. Acquisition of the Relevant Parameters

Bee Gaik Yew
Dept. of Civil and Environmental Engineering, The University of Tennessee, Knoxville, TN 37996
and
Div. of Chemical Sciences, Oak Ridge National Laboratory, Oak Ridge, TN 37831

Eric C. Drumm
Dept. of Civil and Environmental Engineering, The University of Tennessee, Knoxville, TN 37996

Georges Guiochon
Div. of Chemical Sciences, Oak Ridge National Laboratory, Oak Ridge, TN 37831
and
Dept. of Chemistry, The University of Tennessee, Knoxville, TN 37996

The efficiency of chromatographic columns is adversely affected by large-scale radial variations of the packing density or void ratio of the material used to prepare the bed. This heterogeneity is due to wall friction effects that take place during the preparation of the column and to seepage effects operating during the packing process and the subsequent operation of the column. The dependence of the bed's void fraction on the stress applied during its consolidation was determined, as well as its permeability at various stages of the consolidation process and the coefficient of friction between typical packing materials and the stainless steel wall of chromatographic columns. These results are required to develop and use numerical models of the volumetric response to axial compression of the bed and models of the coupled mechanical-seepage rheology of particulate materials.

Introduction

Even though most tend to ignore it, chromatographers have long known that columns are not radially homogeneous (Baur et al., 1998; Baur and Wightman, 1989; Bayer et al., 1989, 1995; Eon, 1978; Farkas et al., 1994, 1996, 1997; Farkas and Guiochon, 1997; Guiochon et al., 1997; Horne et al., 1966; Knox et al., 1976; Tallarek et al., 1995, 1996). This is true for columns packed with dry (Eon, 1978; Horne et al., 1966; Knox et al., 1976) or wet techniques (Baur et al., 1988; Baur and Wightman, 1989; Bayer et al., 1989, 1995; Farkas et al., 1994, 1996, 1997; Farkas and Guiochon, 1997; Guiochon et al., 1997; Tallarek et al., 1995, 1996), for analytical (Baur et al., 1988; Baur and Wightman, 1989; Bayer et al., 1989, 1995; Eon, 1978; Farkas et al., 1994, 1996, 1997; Farkas and Guiochon, 1997; Guiochon et al., 1997; Horne et al., 1966; Knox et al., 1976; Tallarek et al., 1995, 1996) and for preparative columns (Farkas et al., 1997; Farkas and Guiochon, 1997; Guiochon et al., 1997). Although little has been done about this situation for the past 30 years, the potential reward for a successful breakthrough in packing technology remains important: a doubling of column efficiencies at constant length is a distinct possibility, if we only knew how to pack radially homogeneous columns. Typical reduced HETP measured under favorable circumstances (at near optimum flow rate, with a compatible sample and phase system, using an instrument

Correspondence concerning this article should be addressed to. G. Guiochon.
Current address of B. G. Yew: GZA GeoEnvironmental Inc., One Edgewater Drive, Norwood, MA, 02062.

causing a small amount of extra-column band broadening) are, at best, of the order of 2.0 to 2.5. In contrast, values of the reduced plate height of 1 or less were consistently reported in the literature under two particular sets of experimental conditions. First, this low value was observed for columns that are homogeneous in the radial direction because the ratio of the column diameter to the average size of the packing particles is of a few units (Giddings and Fuller, 1962). In this case, there cannot be a systematic trans-column variation of the mobile phase velocity that cannot be averaged quickly by eddy dispersion. Second, the same result was derived from local measurements of axial band broadening made under such conditions that only the classical phenomena of axial dispersion and mass-transfer resistances are effective, as is the case in NMR (Tallarek et al., 1995, 1996) or optical visualization (Broyles et al., 2002). The lower efficiency derived from measurements made by bulk detection under the same conditions is explained by the warping of the solute bands arising from the large-scale, systematic radial variation of the mobile phase velocity (Bayer et al., 1989, 1995; Farkas et al., 1997; Farkas and Guiochon, 1997; Tallarek et al., 1995, 1996; Broyles et al., 2002). Therefore, it is worthwhile to investigate the mechanisms through which columns become radially heterogeneous during the preparation of their bed.

The state of the art in column packing was reviewed recently (Guiochon et al., 1997). Since then, direct observations have demonstrated that there is friction between the column bed and its wall (Guiochon et al., 1999). This result validated the earlier conclusions of the review regarding the origin of the radial heterogeneity of the column bed. It is consistent with all the observations reported above and with the earlier general results obtained by Train regarding bed consolidation (Train, 1956, 1957). Friction of the bed against the column wall, however, cannot be isolated and the rheology of the bed during its preparation must be studied as a whole. For chromatographers, the rheology of particulate beds is a new and difficult field (Lightfoot, 1999). We summarize here some of the main conclusions.

The behavior of a mass of small particles has little in common with that of either a liquid or a single solid of similar mass, as demonstrated by various simple observations (Jaeger et al., 1996). The behavior of bulk granulated materials is studied in soil mechanics (sands, silts) (Bardet, 1997; Jumikis, 1969; Lambe and Whitman, 1979; Taylor, 1948; Visser, 1965) and in the mechanics of their storage and handling (such as sand, cement, flour, corn) (Jenike, 1964; Schwedes and Schultze, 1990; Tomas, 1993, 1997). Although the amounts handled in the corresponding applications are huge compared to the content of the largest preparative columns, the results are relevant to our purpose. The behavior of powders is also studied in ceramics and in pelleting (such as in pharmaceuticals manufacturing), but with the purpose of these last processes being to turn a mass of particles into one single large object, the green body or the pellet, respectively, the stress level used is high. Also, most particles are broken and fused (Train, 1956, 1957), rendering these studies irrelevant to the behavior of chromatographic beds. Finally, we note that the size of the particles of typical packing materials is usually much smaller and their size distribution is always narrower than those of the materials considered in soil mechanics, or in most storage and handling applications. As a consequence, the external porosity of chromatographic beds (that is, the fraction of the bed volume unoccupied by the particles) is larger (about 0.40) than that of sand beds (which may be as low as 0.20).

There are strong interactions between each particle of a bed and all its neighbors. These particles cannot move freely, as their motion is limited by steric hindrance and by friction between the particles in contact. It is impossible to take all these effects into account. In civil engineering, investigations of the stress-deformation response of soils and the seepage or flow of groundwater through earth embankments and dams are traditionally conducted assuming that the assembly of soil particles can be treated as a deformable, porous continuum (Lambe and Whitman, 1979; Taylor, 1948). This approach is usually justified because the particle size is very small relative to the size of the problem domain. Likewise, because the size of the particles in a chromatography column is small relative to the dimensions of the column, or the number of particles is great, the study of the distribution of the stresses and the flow in a column bed can be made only assuming that the packing material can be represented by a continuum with equivalent material properties. In this work, we assume that integration volumes are large compared to one particle but small compared to the column volume, which is physically acceptable. (The number of particles is great assuming an external porosity of 0.40 gives 2.0 mL for the total volume occupied by the actual particles contained in a 0.46×20 cm analytical column. The volume of a 5 μm particle is 65×10^{-12} mL. Accordingly, there are approximately 30 billion particles in this analytical column.) Then, the particulate bed can be considered as filled with a continuous material, as a true solid (albeit one permeable to a fluid), but a material having physico-chemical and mechanical properties which are functions of the local coordinates. The process during which a slurry solvent bed of particles settle under an external mechanical stress (such as during the packing of a chromatographic column) is called consolidation. We discuss successively the equilibrium state eventually reached at the end of consolidation and the kinetics at which the system tends toward equilibrium.

Several facts well established in solid mechanics are important. The local stress is a function of the direction or the plane on which the stresses are examined. Furthermore, at a given point in the bed, it is not the same in the axial and the transverse direction; fluid pressure, which is a state of equal stress in all directions, is a special case of the general state of stress in a solid. The local stress, which varies with the local position, is given by a matrix. In the case of a point away from the wall of a reasonably well packed column, one of the eigenvectors of the matrix defining the local stress tends to be parallel to the column axis and another one tends to be perpendicular to the axis. However, local fluctuations of these orientations take place and shear stresses exist near the column wall.

The relationship between the state of stress and the state of strain or deformation is described by a constitutive relationship. For the case of a linear elastic material in which the strain is proportional to the stress, this relationship is Hooke's law (Lambe and Whitman, 1979). Nonlinear elastic relationships may be used to describe materials for which the stress and strain are not linearly related. A material which behaves

elastically is one in which the deformation will be completely recovered upon the removal of the stress, much like an elastic band. Many materials are assumed to behave elastically up to yielding or failure, at which time nonrecoverable or plastic deformations occur. For columns packed with silica-based materials, the particles can be assumed to behave in a nonlinear elastic manner up to the point where particle breakage begins to take place, after which plastic response can be assumed. In practice, there is particle breakage only under high compression stress, which should be avoided in practical operations (Guiochon et al., 1997) and will typically only occur in localized regions of the column. With polymer-based particles, the situation is more complex. Large levels of local strain in these materials is probable, causing significant plastic deformation of the particles, accompanied by a decrease in the bed permeability. This explains in large part the aggressive hostility of some manufacturers to the use of high-pressure liquid chromatography (Sofer and Nyström, 1989). The problems associated with the consolidation of beds of polymeric materials will not be further discussed here. Be as it may, the local strain, like the local stress, is a function of the spacial coordinates and varies across the column. As the local external porosity (fraction of the column volume unoccupied by the particles) is directly a function of the local strain, the problem of the column bed heterogeneity is explained by the heterogeneous distribution of the local stress. Solid mechanics may help by providing relationships between local stress and strain.

The strain level in a bed of particles develops and stabilizes during consolidation of the bed under a certain stress. Consolidation involves several parallel phenomena, the compression of the individual particles (negligible for silica), the compression of the particle network (the most important phenomenon in our case), the compression of the liquid phase impregnating the bed (negligible in chromatography (Martin et al., 1973)), and the migration of the mobile phase escaping from the interstitial voids between the particles. The excess mobile phase initially contained in these voids, of which the volume is reduced by the compression of the particle network, flows out under the influence of a transitory hydraulic pressure gradient (Lambe and Whitman, 1979; Taylor, 1948). The last one of these phenomena is important, because it was shown by Terzaghi (1925) to control the kinetics of consolidation of large volumes of soils (Lambe and Whitman, 1979; Taylor, 1948). After Terzaghi (1925) and Taylor (1948), the extent of the consolidation achieved is approximately 93% after a time t such that

$$T = 4\frac{k(1+e)}{a_v \eta L^2} t = 1.0 \qquad (1)$$

where e is the void ratio of the bed, with $e = \epsilon_e/(1-\epsilon_e)$ and ϵ_e as its external porosity, a_v is the compressibility of the bed, with $a_v = de/dp$ (with p, mechanical stress), k is its permeability, L is its length, and η is the dynamic viscosity of the liquid phase (see Guiochon and Sarker (1995), Figure 5). It was shown, however, that under the experimental conditions typically used in liquid chromatography, consolidation kinetics is fast. For a 25 cm long column packed with 15 μm particles of silica (IMPAQ, BTR Separations, Wilmington, DE), it was found that $k = 2.67\times10^{-9}$ cm^2, $e = 0.64$, and $a_v = 2.69\times10^{-9}$ g/cm^2. Hence, for a water/methanol (60:40) solution with $\eta = 1.8$ cP at 20°C, we have $t = 90$ s for $T = 1$ (Guiochon and Sarker, 1995). This result agrees with the common observation that column beds consolidate rapidly under stress (Guiochon et al., 1999; Guiochon and Sarker, 1995; Sarker et al., 1996). This means that the kinetics of the last one of the effects listed earlier, the expulsion of the mobile phase from the consolidated bed takes place rapidly in chromatography, faster than it is usually in soil mechanics because of the high porosity of the column bed and of its small dimensions. The second phenomenon, the compression of the particle network, has the strongest influence on the consolidation in the packing of chromatographic columns.

Consolidation is never instantaneous. Its rate varies markedly from one packing material to the next. It is much faster and more uniform for spherical particles than for irregularly shaped ones (Sarker et al., 1996). For the latter materials, a sharp friction noise may even be heard during consolidation. This noise is not necessarily associated with significant particle breakage (Sarker et al., 1996). It is more probably explained by slippage of the particles against each other. Even for spherical particles, consolidation is not always continuous. Metastable states are not infrequent (Guiochon et al., 1999; Guiochon and Sarker, 1995; Sarker et al., 1996; Stanley et al., 1996). They may last a few minutes to a few hours. After a compression-stress increment is applied, there is not always uniform and smooth reordering of the particles, but an irregular, chaotic succession of local buildup of stress between groups of particles, leading to a local rupture of the equilibrium, with grains rolling over each other or being separated abruptly by a local avalanche of grains resulting from the breakup of a bridge at some distance (Lambe and Whitman, 1979). Although this effect is always observed and often important with irregular shaped particles, it is minor with spherical particles (Guiochon and Sarker, 1995; Cherrak et al., 2001). As a consequence, consolidation tends toward a limit, following a quasi-exponential decay with a pseudo time constant which may be on the order of hours for a small preparative column, but tends to increase with increasing bed volume. Consolidation experiments are never entirely completed. It is common to observe a slow, small shrinkage of a column bed during measurements made over periods of several weeks, even though consolidation seemed to have been completed within the first few minutes of the bed compression (Guiochon et al., 1999).

While the first consolidation of a newly packed column bed is accompanied by an important and irreversible decrease in its length, further consolidations after unloading are nearly reversible (Cherrak et al., 2001; Guiochon et al., 1999; Guiochon and Sarker, 1995; Sarker et al., 1996; Stanley et al., 1996) and follow the law of elasticity, as expected for these particulate materials. This result is a classical one in soil mechanics (Bardet, 1997; Jenike, 1964; Jumikis, 1969; Lambe and Whitman, 1979; Taylor, 1948; Visser, 1965). Figure 1 shows an idealization representation of the stress-strain response of a sand bed (see discussion in the Theory section).

Using the fundamental results of solid mechanics, soil mechanics has developed the tools required for the modeling of the consolidation behavior under stress of beds of actual

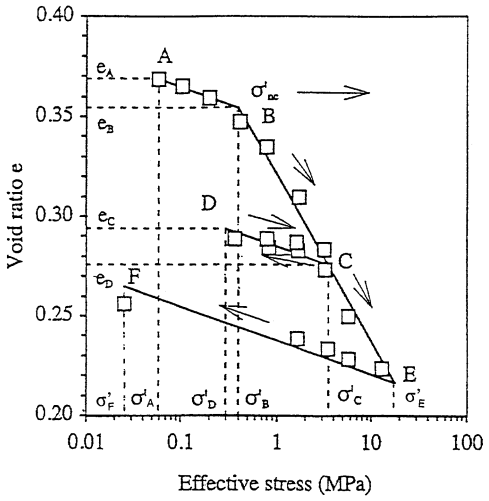

Figure 1. Idealized representation of the stress–strain response (Bardet, 1997).

granulated materials having their external pores entirely filled with a fluid (the mobile phase in chromatography). In practice, the internal pores will also be filled with the same fluid, but this is irrelevant for the present work because the particles are so rigid that their volume is not significantly affected by the stress applied to the bed. (The Young modulus of silica is 72 GPa (Bansal and Doremus, 1986). Under a uniform compression stress of 10.0 MPa, the particle dimensions would shrink by approximately 0.014%.) Although the mathematical framework required to model the nonlinear stress-strain response of these materials and the time rate dissipation of the pressure in the fluid-filled voids has long been available, the solution of the problem is complex because the relationships involved are not linear. Numerical approximations, such as the finite-element methods of Zienkieweicz (1971), and Desai and Abel (1972), can be utilized to calculate both the distribution of stress and that of strain in a bed. To afford realistic results, however, these methods require the availability of accurate values of the relevant parameters which characterize the behavior of the materials studied under stress. These parameters include the internal angle of friction of the packing material, the coefficient of friction of the bed against the wall, the void fraction of the bed, its permeability under different homogeneous stress levels, and the elastic constant of the consolidated material. This article reports on the determinations of these parameters for two materials typical of those used in preparative liquid chromatography. In the second part of this article, the results obtained in the modeling of the behavior of column beds will be discussed (Yew et al., 2003).

Theory

Definitions of the parameters used

The correlations used in soil mechanics are based on the consideration of the void ratio e (Bardet, 1997; Lambe and Whitman, 1979; Taylor, 1948). This parameter is similar to the phase ratio F used in preparative chromatography (Guiochon et al., 1994), but it refers only to the volume accessible to the fluid percolating through the bed. The *void ratio* is given by

$$e = \frac{\epsilon_e}{1-\epsilon_e} \tag{2}$$

The *external porosity* ϵ_e is defined as the fraction of the column volume available to the mobile phase percolating through the bed (the fluid in the pores which are inside the particles are excluded).

Loading, unloading and reloading processes

Figure 1 shows the consolidation curve or stress-strain plot of a typical fine-grained material under a uniaxial strain loading. The stress-strain response of particulate materials is usually described in terms of the effective stress σ', which is the difference between the total applied stress and the pressure in the fluid-filled voids. The relationship between the void ratio e and the effective stress is nonlinear and irreversible. The material behaves differently during the first loading (path ABCE) or during reloadings (such as path FE). Paths ABCD and DCEF illustrate, first, a loading under a limited stress (σ'_C) followed by unloading to σ'_D, secondly, a reloading to σ'_C and a further loading to σ'_E, and, finally, an unloading to σ'_F. The material response illustrated in Figure 1 is not elastic, but is elastoplastic. Starting from point A, the void ratio e varies linearly with log σ' when σ' is increased from σ'_A to σ'_B

$$e = e_A - C_s \log \frac{\sigma'}{\sigma'_A} \tag{3}$$

where C_s is the *swelling index*, e_A is the void ratio at point A, and σ'_A is the effective stress at point A. Equation 3 is valid until σ' reaches the stress threshold σ'_B, at which point the e-σ' curve becomes abruptly steeper than along the branch AB. When $\sigma' > \sigma'_B$, the void ratio e varies again linearly with log σ', but with a steeper slope

$$e = e_B - C_C \log \frac{\sigma'}{\sigma'_B} \tag{4}$$

where C_C is the compression index, e_B is the void ratio at point B, and σ'_B is the effective stress at point B.

When σ' is decreased from σ'_C to σ'_D, the point representing the stress and strain of the bed ($e - \log \sigma'$) migrates along the unloading branch CD, which is parallel to AB and has a slope equal to the swelling index. The correlation equation becomes

$$e = e_C - C_s \log \frac{\sigma'}{\sigma'_C} \tag{5}$$

When σ' is increased again, the point ($e - \log \sigma'$) follows the reversible path DC, now from D toward C and then toward E, on the branch that extends BC. When σ' is finally decreased from σ'_E to σ'_F, the point ($e - \log \sigma'$) follows the branch EF, parallel to AB and DC. The branch BCE is called the *virgin compression line* or VCL. The branches AB, DC and FE are called *swelling lines*. A particular material has only one virgin consolidation curve, but may have an infinite number of swelling branches or lines. The swelling branches

are always on the left of the VCL. The point ($e - \log \sigma'$) cannot be located on the right of the VCL.

The stress-strain relations given in Eqs. 3–5 are nonlinear because the strain e is a logarithmic function of the stress σ'. They are also irreversible, because it is not possible to return to point A once σ' has exceeded σ'_B. The threshold of irreversibility is defined by the largest effective stress applied during the previous history of the block of material studied. It is referred to as the pre-consolidation pressure σ'_P. When the stress state is smaller than σ'_P, the response is initially described by a swelling branch (as long as $\sigma'_P > \sigma'$). When the stress state is equal to σ'_P, the response follows the VCL for further loading and a swelling line for unloading. The pre-consolidation pressure σ'_P either increases or remains constant during any further work done with a given bed, but it can never decrease. During the loading ABC in Figure 1, σ'_P increases from σ'_B to σ'_C. σ'_P is constant during the unloading CD and the reloading DC, but increases again during the loading CE.

Permeability of porous media

The mobile phase percolates through beds of packing materials at a velocity which is proportional to their permeability. Chromatographers, chemical engineers, and hydrogeologists use the *permeability* or intrinsic permeability, k dimension L^2, defined in Darcy's law (Bird et al., 1960; Freeze and Cherry, 1979)

$$k = \frac{\eta u L}{\Delta P} = \frac{\mu u L}{\Delta P \rho g} \tag{6}$$

where η is the viscosity of the mobile phase, μ (M/LT) is its dynamic viscosity ($\mu = \eta\rho g$, with ρ density of the mobile phase and g (L/T^2) gravitational constant), u is the mobile phase velocity under the inlet or head pressure ΔP, and L is the bed length. Since, in a porous material, k (dimension L^2) is related to the pore volume which is in turn related to the solid volume, k is often assumed proportional to the square of the average size of the particles of the packing material (Bird et al., 1960; Freeze and Cherry, 1979; Bardet, 1997).

In civil engineering, the permeability is usually expressed in terms of the hydraulic conductivity K dimension L/T, which depends on both the packing material and the fluid, usually water. It is related to the permeability by (Freeze and Cherry, 1979)

$$K = \frac{k \rho_w g}{\mu} \tag{7}$$

where ρ_w is the density of the fluid (water). The permeability of a bed of packing material can be measured during its consolidation, using the falling head test (see Experimental Studies section).

The Kozeny-Carman equation (Bird et al., 1960; Freeze and Cherry, 1979) is an empirical correlation used to estimate the permeability from the void ratio (Bardet, 1997)

$$k = \frac{\mu}{\rho_w g} \frac{Y_w}{5 f \mu S^2} \frac{e^3}{1+e} = \frac{1}{5 f S^2} \frac{e^3}{1+e} = \frac{1}{5 f S^2} \frac{\epsilon_e^3}{(1-\epsilon_e)^2} \tag{8}$$

where k is the permeability, Y_w is the weight of liquid per unit volume, the parameter f depends on the shape of the extraparticle pores through which the mobile phase percolates ($f = 1.1$ for spherical particles, $f = 1.25$ for quasi-spherical particles, and $f = 1.4$ for irregular particles (Loudon, 1952), and S^2 is the average external specific surface area of the particles, with the surface responsible for the viscous friction between the bed and the mobile phase. S is often determined by (Bardet, 1997)

$$S = \frac{6}{\sqrt{d_{\max} d_{\min}}} \tag{9}$$

where $d_{\max}$ is the dimension of the largest particles and $d_{\min}$ is that of the smallest ones. In practice their product may be replaced by $d_{90}\ d_{10}$ where d_{90} and d_{10} are the sizes below which 90% and 10% of the particles are found, respectively.

Shear Stress at the Interface between Packing Material Bed and Steel Wall

Beds of silica particles, like any material object, fail at some point when subjected to an increasing shear stress. This shear-stress threshold is called the *shear strength* of the material. A material cannot withstand a shear stress larger than its shear strength, and it may deform extensively when the applied shear stress approaches its shear strength. It turns out that the interface of contact between two materials has a shear strength as well. If the interface is rough, the shear strength may be greater than that of the weaker material, and the plane of failure or slip will migrate into the weaker material (the shear strength of the weaker material will then govern interface slip). If the contact is smooth, such as that between a bed of consolidated silica particles and the steel wall of the column, the interface has a shear strength lower than that of the bed itself and will fail first. The bed will slip along the wall when the shear stress equals the shear strength of the interface. This shear strength or the corresponding coefficient of friction between the packing material and the column wall is an important factor in an investigation of the packing process.

The shear strength of the interface between the packing material and the column wall can be measured in a direct shear test designed to reproduce the conditions during the column packing and operation. This direct shear test is illustrated in Figure 2. The silica sample is confined inside a rigid cylindrical sample ring, and subjected to a normal load N, after which a shear force T is applied. If A is the area of the contact surface along plane CD, the shear stress τ_{xy} acting on the contact surface is equal to T/A, and the normal stress σ_y is equal to N/A. For a cylindrical box, we have

$$A = \frac{\pi D^2}{4} \tag{10}$$

where D is the diameter of the sample box. The shear stress at failure is observed to increase with increasing applied normal stress, which is indicative of a frictional material. For a given value of the normal stress σ_y, the shear-strength of the silica sample is the shear stress τ_{xy} that causes the sample to fail or slip along the plane CD (that is, the horizontal sur-

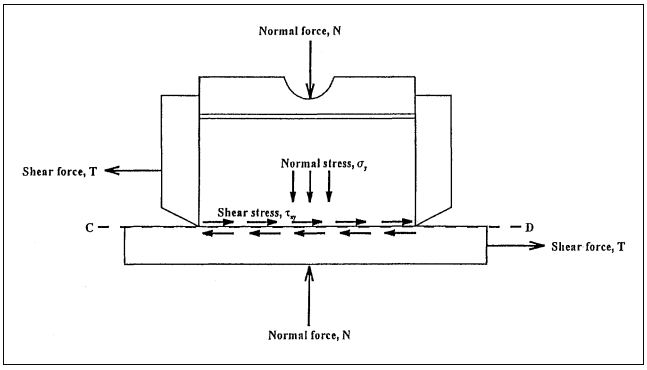

Figure 2. Shear strength at the steel-packing material interface.

Forces and stresses applied to a silica sample in the shear box.

face), which is represented by point M in the Mohr-Coulomb diagram (Bardet, 1997; Lambe and Whitman, 1979; Taylor, 1948) shown in Figure 3. The relationship between the normal stress and the shear stress at failure is often assumed to follow a linear relationship (see Figure 3) as

$$\tau = \boldsymbol{C} + \sigma \tan \delta \tag{11}$$

where $\boldsymbol{C}$ is the cohesion and δ is the interface friction angle. This angle, which is used to describe the strength of the interface, is analogous to the internal friction angle ϕ, which is used to describe the strength of the material itself. If the cohesion is small or zero, the tangent of the friction angle is alternately referred to as the coefficient of friction.

During the direct shear test, the stress state is not completely defined, except at failure: the stresses are known only on the horizontal surface at failure (σ_y and τ_{xy}) and the other stresses are unknown in all other planes. If the shear stress on the horizontal plane τ'_{xy} is measured at a larger value σ'_y of the normal stress, the stress at failure is represented by point M′ in Figure 3 and the linear failure envelope AMM′ can be drawn. Adoption of the Mohr–Coulomb failure criterion assumes that the Mohr circle is tangent to the failure surface, and that the point of contact corresponds to the stresses on the failure plane at failure. This allows the construction of the Mohr circle at failure (Figure 3). The Mohr circle at failure is tangent to AMM′, and its center B is given by line MB perpendicular to AM. Thus, the Mohr circle can only be drawn at failure, once the failure envelope has been determined. As shown in Figure 3, point M represents the stress on the horizontal surface (the failure surface), and point N represents the stress on the vertical surface. The stresses on any other plane can be determined graphically from the Mohr circle by drawing a line from point P, referred to as the "Pole" or origin of planes (Lambe and Whitman, 1979), oriented in the plane of interest. The point where this plane intersects the Mohr circle will determine the normal and shear stresses on that plane.

Application to tilt tests

These tests were carried out to compare the interfacial friction between a block of a phenolic material and a steel plate coated with various lubricants (to assess the potential interest of lubricating the column wall prior to packing the column, see Yew et al., 2002). Consider the block of weight W resting on a plane surface which is inclined at an angle α to the horizontal surface. The block is acted upon by gravity

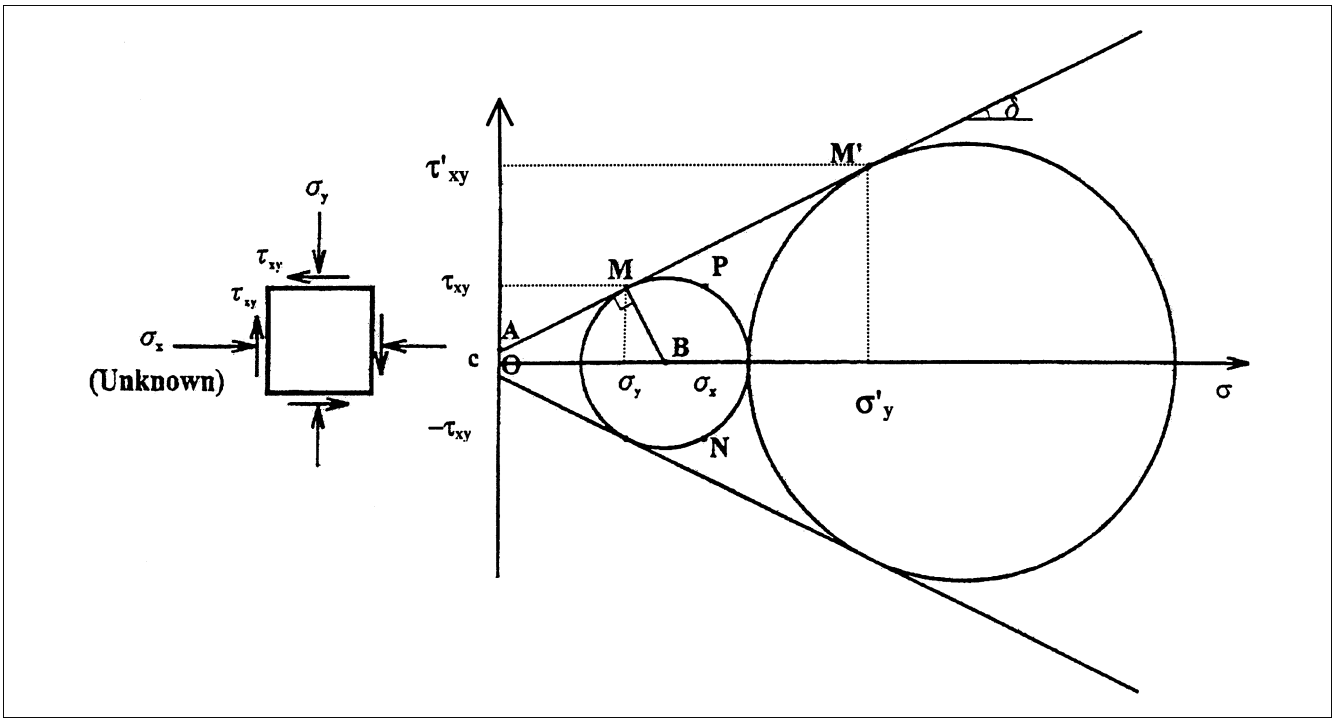

Figure 3. Stress state at failure in the shear stress box and its Mohr representation.

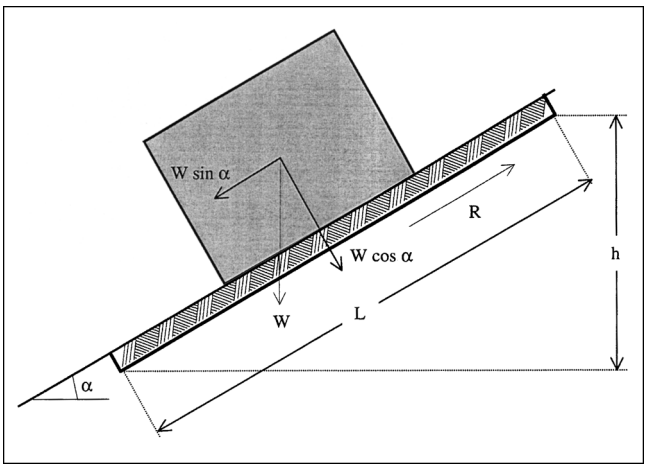

Figure 4. Tilt test.

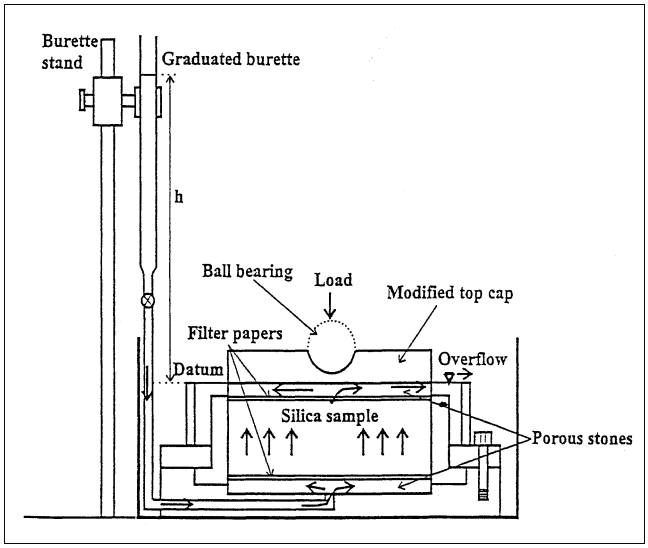

Figure 5. Oedometer assembled with a burette on its side for the falling head permeability test.

only and, hence, its weight W acts vertically downward, as illustrated in Figure 4. The resolved component of W, which acts down the plane and tends to cause the block to slide along it, is $W \sin \alpha$. The component of W which acts across the plane and tends to stabilize the block by causing friction is $W \cos \alpha$. The normal stress σ, which acts across the potential sliding surface, is given by

$$\sigma = \frac{W \cos \alpha}{A} \tag{12}$$

where A is the base area of the block. The relationship between the shear strength of the sliding surface and the normal stress is given also by Eq. 11, where τ is the shear stress, σ is the normal stress, and δ is the interface friction angle. Substituting for the normal stress from Eq. 12

$$\tau = \left[\frac{W \cos \alpha}{A} \right] \tan \delta = C \tag{13}$$

so, the resisting force τA that prevents the block from sliding is given by

$$\tau A = W \cos \alpha \tan \delta + CA \tag{14}$$

The block will be just on the point of sliding or in a condition of limit equilibrium when the force acting down the plane is exactly equal to the resisting force, hence

$$W \sin \alpha = W \cos \alpha \tan \delta + CA \tag{15}$$

If the cohesion $C = 0$, as is the case for the packing material-steel interface that is investigated in the direct shear tests reported here (see later), the condition of limit equilibrium defined by Eq. 15 reduces to

$$\alpha = \delta \tag{16}$$

$$\delta = \sin^{-1}\left(\frac{h}{L} \right) \tag{17}$$

Thus, the angle at which the block begins to slide is the interface angle of friction δ between the two materials. By measuring the height of the plate h when the block starts to slide and knowing the plate length L, the interface friction angle can be derived simply from Eq. 17.

Experimental Studies

Equipment

Consolidation: Oedometer. An oedometer was used to determine the compression index C_c, the swelling index C_s, the preconsolidation pressure σ_p' (which defines the compressibility of the packing material), and the coefficient of consolidation C_v (which characterizes the rate of primary consolidation) (Bardet, 1997; Yew, 1999; Holtz and Kovacs, 1981). This instrument is conventionally used in soil mechanics for this purpose. Its design is illustrated by Figure 5.

The heart of the instrument is a stiff 2.5 in. (6.25 cm) ID ring, filled with the material under study. The ring prevents lateral expansion of the sample of material which is enclosed between two porous, flat stones. The stones are permeable, allowing drainage of the solvent located in the external pores when the particle network is compressed and strained. A beam-and-counter-weight mechanism is used as the loading device to apply and maintain the axial load to the sample. A dial indicator with a range of 0.5 in. (12.7 mm) and an accuracy of 0.0001 in. (2.54 μm) is attached to the top of the modified cap, to measure the vertical displacement of the sample as a function of time.

Permeability. The permeability of the packing materials was measured by conducting a falling-head permeability experiment at the end of each consolidation step, before applying a new loading increment. Figure 5 shows the instrument used to measure the permeability during the consolidation tests. In practice, it is integrated in the oedometer. The sample in the rigid container is squeezed by a constant vertical load. The standpipe consisting of a graduated burette is attached to the side of the consolidation cell. It contains methanol which flows through the sample and the porous

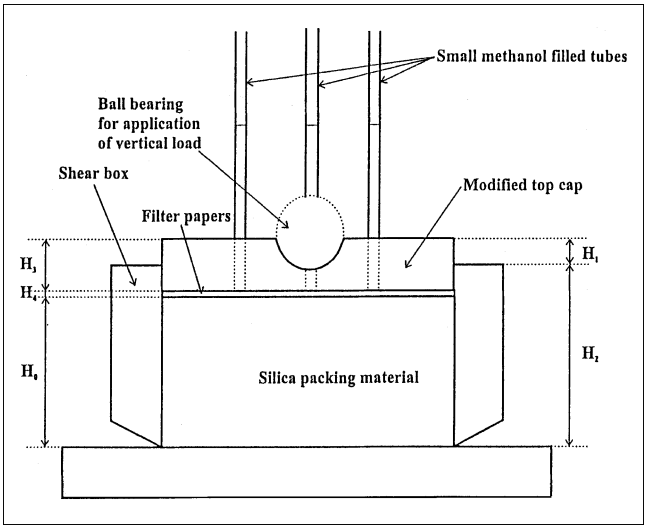

Figure 6. Apparatus used for determining the shear stress of the interface between consolidated bed of packing material and steel plate.

stones, from the bottom up, under a certain head pressure (see Experimental Procedures).

Shear Stress. A standard direct shear test apparatus modified for interface testing was used (Figure 6). A shear box with an ID of 63.5 mm is in contact with a polished stainless steel plate. A top cap slides smoothly into the box. A ball bearing mounted on the top cap allows the application to the sample of a known stress perpendicular to the surface of friction. The edge of the shear box in contact with the sliding plate are sharpened to reduce the contribution of the steel wall to the friction coefficient. Dial gauges measure the lateral and vertical displacements of the shear box which are recorded.

Materials

Two common packing materials were used in this study, Zorbax (BTR Separations, Wilmington, DE, now Agilent Technologies, Palo Alto, CA), a quasi-spherical C18-bonded silica and Kromasil (Eka Nobel, Bohus, Sweden), a spherical C8-bonded silica. Both samples were obtained in 1995–1996 and may not be representative of the current fabrication. Micrographs of these materials are shown in Figure 7. Note that the magnification in each photograph is different. The average particle diameter of both materials is about 10 μm (which is approximately the average size of silt particles often encountered in soil mechanics). Values of 14 and 12 μm for d_{90} and of 7 and 8 μm for d_{10} were found for Zorbax (Figure 7a) and Kromasil (Figure 7b), respectively. Unlike those of Kromasil, the Zorbax particles are not truly spherical particles. A fraction of them are agglomerates of a few spherical particles, as shown in Figure 7a.

Methanol (density, 0.791 g/cm^3, viscosity, 0.55 cp) and acetone (density, 0.790 g/cm^3, viscosity, 0.32 cp) were purchased from FisherChemicals (Pittsburgh, PA). The interface lubricants used in some shear tests were Sprayon (McMaster-Carr, Atlanta, GA) sprays, suspensions of particles of powder and flake graphite, Teflon, and Boron Nitride (a ceramic) in a volatile solvent.

Experimental Procedures

All the measurements of the properties of the beds of the packing material studied are made by filling sample cells with a slurry of the packing material and consolidating the slurry into a bed, essentially following the same process as used in the packing of chromatographic columns. The question then arises of the degree of homogeneity of the material in the test cells used to measure its properties. We assume that the beds of packing material prepared in the sample cells are homogeneous, and we will use the parameters measured to predict the degree of heterogeneity of the columns. The reason why our approach is valid is to be found in the difference between the aspect ratios of the beds in the columns and in the sample cells. Columns for preparative liquid chromatography are between 5 and 80 cm in diameter and between 20 and 80 cm in length. Their aspect ratio is commonly between 4 and 1. The sample cells used are 6.25 cm wide and 2.3 cm

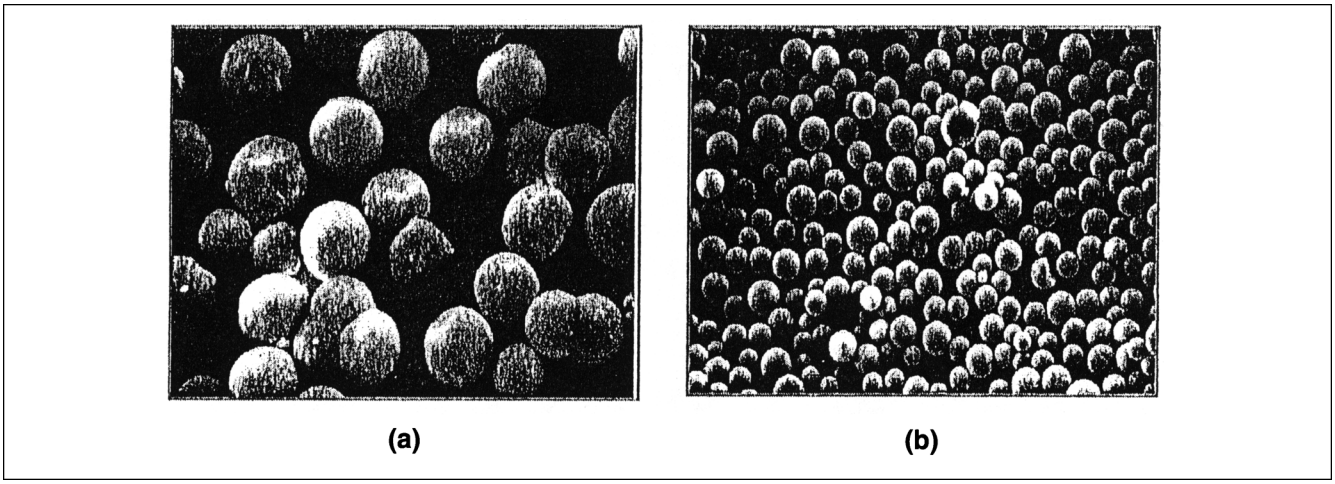

Figure 7. Micrographs of the two packing materials.
(a) Zorbax; (b) Kromasil.

thick; hence, an aspect ratio of 0.35. It is commonly accepted in soil mechanics (Potyondy, 1961; Jenike, 1964; Bardet, 1997) that samples in cells having an aspect ratio below 0.5 can be considered as homogeneous, that the wall friction of the shear cell has negligible effect, that the void fraction is homogeneous, and that the stress is homogeneously distributed both axially and radially in the cell.

Consolidation of Packing Materials. A slurry was prepared by mixing 50 g of the packing material and 125 mL of methanol. It was stirred for approximately an hour to ensure that all the particles were properly dispersed, wetted, and degassed. The slurry was then poured carefully into the oedometer. The slurry sample was allowed to settle and the supernatant excess of methanol was taken away with a large syringe. Two sheets of filter paper were placed against the porous stones, above and below the sample, in order to separate the silica particles from these porous stones. The top cap was placed on the top porous stone, and the sample was then completely immersed in methanol so that it remained fully saturated during the whole experiment.

The loading sequence of consolidation experiments depends not only on the materials tested, but also on the engineering application. The duration of each load application depends on the rate of consolidation of the material studied. Ideally, a new, higher load should be applied only after the degree of consolidation has stabilized. In practice, this is not possible. The load is changed at convenient time intervals such that the estimated degree of consolidation exceeds 90%. In the tests made on the packing materials which are reported here, a load increase was applied to the sample every 24 h. This was consistent with laboratory observations that the whole primary consolidation of the sample was well completed after less than 24 h. This is also consistent with observations made in chromatography that the beds are consolidated after less than an hour (Guiochon et al., 1999; Guiochon and Sarker, 1995; Sarker et al., 1996; Stanley et al., 1996; Yew et al., 2003).

Data Measured during Consolidation Experiments. When an axial stress σ is applied to the sample, it deforms vertically and shrinks with passing time. The sample initial height h_0 ultimately settles down by an amount Δh, once the excess of pore methanol is completely drained and the hydrostatic pressure returns to 0 (the hydrostatic pressure of the methanol column is neglected). In other words, the consolidation is complete when the internal effective stress σ' is equal to the externally applied stress σ. The corresponding axial strain ϵ_z is given by

$$\epsilon_z = \frac{\Delta h}{h_0} \tag{18}$$

Since the stiff ring around the sample prohibits any lateral strain (that is, $\epsilon_x = \epsilon_y = 0$), the volumetric strain ϵ_v is, thus, given by

$$\epsilon_v = \epsilon_x + \epsilon_y + \epsilon_z = \epsilon_z = \frac{\Delta h}{h_0} \tag{19}$$

The volumetric strain ϵ_v is also given by

$$\epsilon_v = \frac{V_0 - V}{V_0} = \frac{\dfrac{V_0}{V_s} - \dfrac{V}{V_s}}{\dfrac{V_0}{V_s}} = \frac{e_o - e}{1 + e_0} \tag{20}$$

where e is the void ratio under load σ, e_0 is the initial void ratio, V is the volume of the sample of packing material under load σ, V_0 is its initial volume, and V_s is the total volume of the silica particles, assumed to be noncompressible. Therefore, e is related to Δh through

$$e = e_0 - \epsilon_v(1 + e_0) = e_0 - \frac{\Delta h}{h_0}(1 + e_0) \tag{21}$$

The initial dry density ρ_{d0} and the initial void ratio e_0 of the material under study can be calculated through the following equations

$$\rho_{d0} = \frac{M_s}{V_0} \quad e_0 = \frac{G_s \rho_w}{\rho_{d0}} - 1 \quad V_0 = \frac{\pi D^2 h_0}{4} \tag{22}$$

where M_s is the mass of dry sample used to prepare the slurry and ρ_s is the density of solid silica (2.65 g/cm^3), D is the diameter of the sample holder, h_0 is the initial sample height, G_s is the specific gravity of the packing material ($= \rho_s/\rho_w$), and ρ_w is the density of water.

Permeability Measurements. The measurements of the coefficient of permeability k are made at the end of the consolidation, just prior to the application of a higher compression stress. Percolation of the methanol contained in a burette through the consolidated bed is allowed by turning on the burette tap. The coefficient is derived from readings of the height of the methanol column as a function of time through the relationship (Freeze and Cherry, 1979)

$$K = \frac{aL}{At} \ln \frac{h_0}{h_t} \tag{23}$$

where a is the cross-sectional area of the graduated burette, A is the cross-sectional area of the sample holder, L is the length (that is, height) of the sample bed, and h_0 and h_t are the elevation of methanol solvent in the standpipe above the discharge level at time $t = 0$ and at time t, respectively. Note that K is a hydraulic conductivity, not an intrinsic permeability (as k).

Shear Stress Measurements. A slurry was prepared with 50 g of packing material (solid density, 2.65 g/cm^3) and 125 mL of methanol (density, 0.79 g/cm^3). The slurry was slowly stirred in a blender for approximately one hour, so that the spherical particles of silica were properly dispersed and wetted. Then, it was poured slowly and carefully into the shear box and settlement of the silica sample was allowed. The excess methanol on top of the silica was decanted using a large syringe. A sheet of filter paper was placed between the silica sample and the modified top cap. This prevents the silica from

flowing out of the shear box with the methanol when a compression step is applied to the sample. The methanol flows through the tubes placed on top of the cap, as illustrated in Figure 6. It is important to note that 50 g of packing material in a 63.5 mm diameter shear box give a bed approximately 10 mm high. Accordingly, the bed diameter is large with respect to its height (aspect ratio, 0.16) and friction of the bed against the side wall of the shear box slightly affects the vertical stress applied by the bed to the steel plate against which it slides and the bed is rather homogeneous (Bardet, 1997; Lambe and Whitman, 1979; Taylor, 1948).

The initial height of the sample H_0 (about 10 mm) was calculated by measuring the depth of the shear box H_2, the height of the top cap H_3, the thickness of the filter paper H_4, and the distance H_1 (Figure 6) with a caliper

$$H_0 = H_1 + H_2 - H_3 - H_4 \tag{24}$$

The dial gages that measure the lateral and vertical displacements were then attached to the shear box and the initial reading recorded. An increasing normal stress was applied to the sample at a rate of about 100 kPa (one bar) per hour and the vertical displacement of the top cap was recorded. This rate assumed that the primary consolidation of the sample was completed after one hour, a figure that was found to be consistent with the observations made of the variations of the sample height with passing time in the consolidation test.

Methanol was added to the sample box surrounding the sample to prevent the methanol inside the shear box from evaporating after the initial value of the normal stress was applied.

The volumetric response of the packing material was measured during the application of the normal stress. Then, the displacement-controlled direct shear tests were conducted, the shear box was pushed laterally at a rate of approximately 1.3 mm/min (Bardet, 1997), and the resulting shear resistance of the interface was measured. Displacement-controlled tests are preferred because they yield the residual shear strength, or post-peak shear stress. The shear force and the vertical and horizontal displacements were measured and recorded at every 0.05 mm of lateral displacement (Bardet, 1997). The test was continued until the shear force became constant. The tests were performed at normal stresses of 250 kPa, 500 kPa, 1,000 kPa, 2,000 kPa, and 3,000 kPa. Several replications of the measurements were made at most values of the normal stress.

Tilt Tests. These tests were conducted with a block of phenolic resin and the same steel plate as for the shear tests. The apparatus used is shown in Figure 4. The plate was attached to a machinist's sine plate (also in the figure). One end of the plate was raised by cranking the handle of the sine plate at a constant rate of about 90 mm/min, while the other end was kept immobile. Prior to each test, the steel plate was carefully cleaned, then lubricated by spraying with a suspension of the desired lubricant. The aim of these tests was directly to measure the interface friction angle δ with various lubricants, in order to select the most appropriate lubricant for investigations in the direct shear test.

The lubricants investigated included flake graphite, powder graphite, Teflon, and boron nitride. The solid lubricant, suspended in a volatile solvent, was sprayed slowly and carefully, so that a uniform layer of graphite was applied to the plate. The thickness of the graphite layer was approximately 3.5 μm, as estimated by measuring the mass difference before and after spraying the graphite onto a test slide, and knowing the density of graphite and the area sprayed. The flake graphite gave the best results in the tilt test (see later). For this reason, graphite was selected for further shear tests.

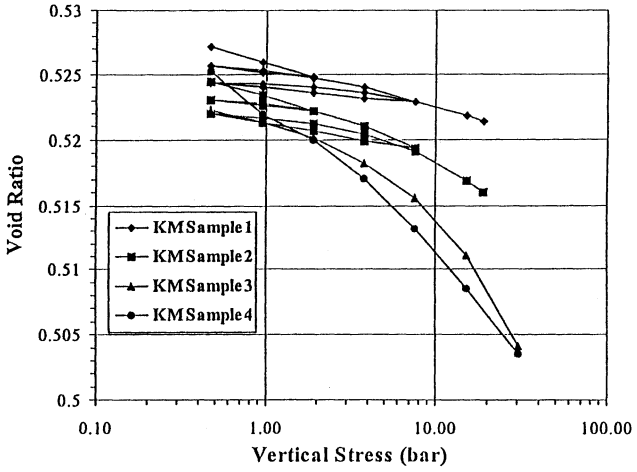

Figure 8. Void ratio vs. vertical stress applied (bar) for two samples of Kromasil C8.

Results and Discussion

Consolidation of Kromasil

Figure 8 shows experimental results representative of the response of Kromasil C8 subjected to a loading-unloading-reloading cycle in the consolidation test. The measurements were made with the material saturated with methanol. The compression index C_c, and the swelling index C_s, which define the soil compressibility for these tests, were calculated and are summarized in Table 1. One important conclusion of this test is that, in the range of stress investigated, Kromasil has a value of the compression index which is much lower than that found for typical geological materials.

Table 1. Compression and Swelling Indices of Kromasil in Methanol

Sample	Compression Index, C_C	Swelling Index, C_S
Kromasil Sample 1	0.0035	0.0013
Kromasil Sample 2	0.0056	0.0022
Kromasil Sample 3†	0.0232	N/A
Kromasil Sample 4†	0.0166	N/A
Avg. of Kromasil Samples 1 and 2	0.0046	0.0018
Poorly Graded Sands*	0.055	0.010
Clay Till**	0.08	N/A
Very Low Plasticity Soils***	0.024	N/A

*As summarized by Holtz and Kovacs (1981).
**As summarized by Bardet (1997).
***Based on the empirical equation: $C_C = 0.75(e_0 - 0.50)$, with $e_0 = 0.5319$ (Holtz and Kovacs, 1981).
†C_C of these samples should not be taken into account in the calculation of an average.
C_C for Kromasil samples, due to the loss of materials during the permeability tests.

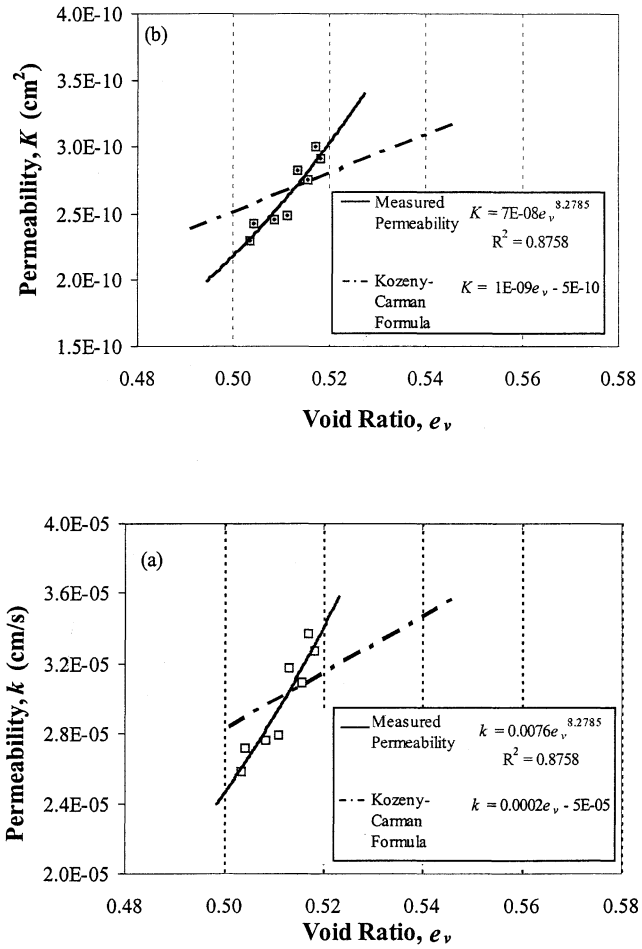

Figure 9. (a) Coefficient of permeability; (b) permeability vs. void ratio for Kromasil C8.

e_v is substituted to e to avoid a possible confusion with a natural exponential.

Permeability of Kromasil

The dependences of the coefficient of permeability (Figure 9a) and the permeability (Figure 9b) of Kromasil C8 consolidated with methanol are shown in Figure 9. As expected, the permeability decreases rapidly with a decreasing void ratio. For comparison, the permeability values obtained using the Kozeny-Carman equation (and Eq. 9 to estimate the effect of the particle size distribution) are also shown in Figures 9a and 9b. This equation appears to give a reasonable estimate of the permeability and of the relationship between the values of the permeability obtained by experimental measurements and those derived from the void ratio. Regression analysis was performed on the data and a power correlation (Figure 9) was found to provide a good approximation of the experimental data. The permeability coefficients of the bed of packing material ranges between 2.6×10^{-5} and 3.4×10^{-5} cm/s, which is close to the typical value for silty sand (1×10^{-5} cm/s) reported by Freeze and Cherry (1979).

Shear strength of bulk packing material

Mihlbachler et al. (1998) measured values $\phi = 36°$ for the internal friction angle of Pro 10 Sil (DuPont, Karlsruhe, Germany, a packing material very similar to the Zorbax material used in this work, except that it is a neat silica, while the material used here is a C18-bonded silica) and $\phi = 23°$ for Kromasil NP 10 (Eka Nobel, Bohus, Sweden, a nonbonded silica material). Both materials were consolidated in the presence of water. These values were assumed to represent the shear strength of the bulk packing material.

Shear strength of the interface between packing material and steel wall

The direct shear test allows the determination of the shear strength of a material along predetermined failure surfaces. In this test, the material response is reported vs. the shear displacement instead of the shear strain because it is impossible to evaluate the shear strain, since the shear strain cannot be defined for a contact surface with zero thickness. The tests were performed at various normal stresses, and several replicate determinations were made at most normal stresses. Figure 10a shows the typical response of the Zorbax material with methanol as the solvent, when subjected to direct shear loading with normal stresses ranging from 250 kPa to 3,000 kPa (2.5 bar to 30 bar). In Figure 10b, the shear stress response is normalized with respect to the applied normal stress,

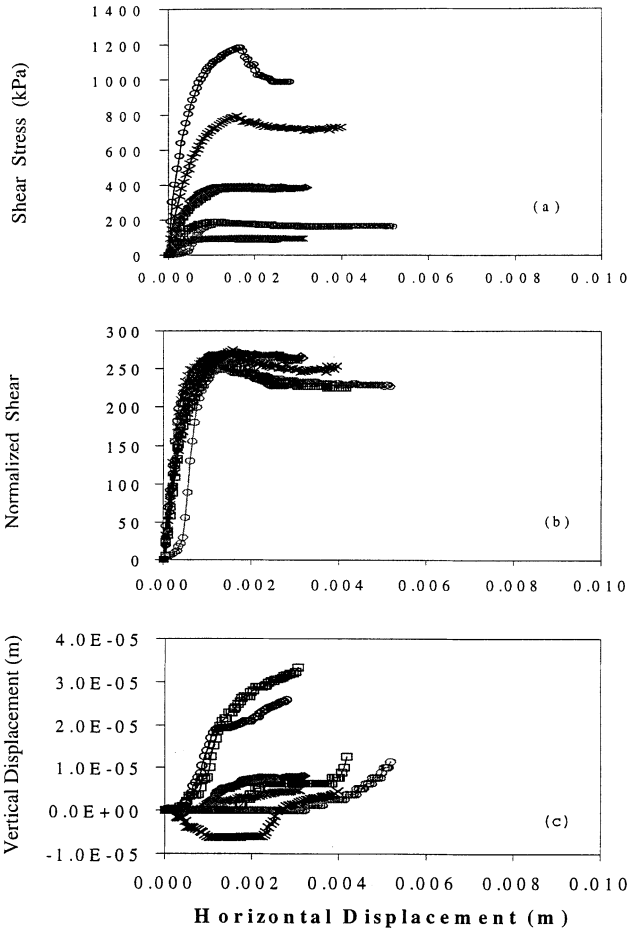

Figure 10. (a) Shear stress; (b) normalized shear stress; and (c) vertical displacement vs. horizontal displacement.

Zorbax material consolidated from a methanol slurry.

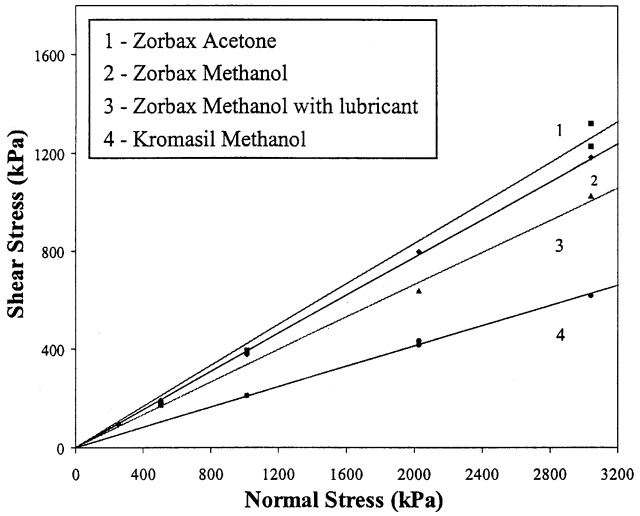

Figure 11. Mohr–Coulomb failure envelopes for the direct shear stress.

Shear stress at failure vs. normal stress, at various bed — steel interfaces.

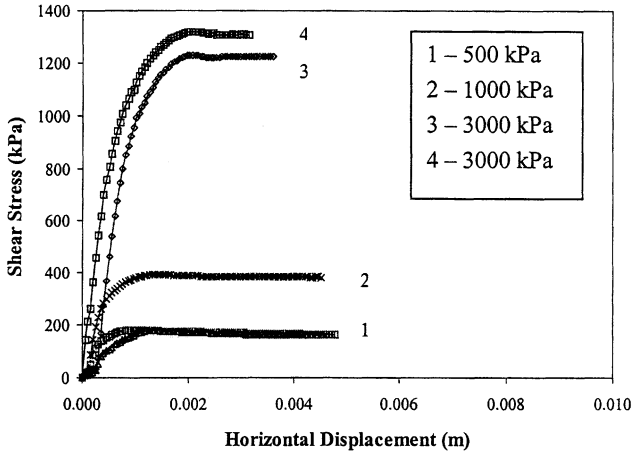

Figure 12. Shear stress vs. horizontal displacement for Zorbax consolidated from a slurry in acetone.

such that differences in the peak response correspond to deviations from the assumed linear relationship between the strength and normal stress. In Figure 10c the variation of the vertical displacement or volume change response is compared as a function of horizontal displacement. With increasing shear (that is, horizontal) displacement, the vertical displacement is observed to increase, which corresponds to an increase in volume or increase in void ratio. This behavior is indicative of a dense particle packing which is becoming more loose during shearing. The peak failure is characterized by the maximum friction angle φ_p. The residual failure is characterized by the residual friction angle φ_r. The peak values corresponding to the shear stress at which slip is initiated are plotted to obtain the Mohr-Coulomb envelope.

The results of this test suggest that the contact between the Zorbax silica sample and the stainless steel plate follows a Mohr–Coulomb failure law with a cohesion $C = 0.0$ kPa, and a friction angle $\delta = 21°$, corresponding to a coefficient of friction tan $\delta = 0.39$, as shown in Figure 11.

Influence of the solvent on the shear strength of interface between packing material and steel wall

(a) Results from Zorbax. Previous results have shown that the stress which needs to be applied to the bed to force it to slide out of the column depends strongly on the nature of the solvent which impregnates the packing material (Guiochon et al., 1999). To evaluate the possible influence of the nature of the solvent on the friction coefficient between the bed in an HPLC column and the wall, an additional series of direct shear tests was conducted. The same method described earlier, in the procedure section (see Experimental Procedures section), was used, except that acetone was substituted for methanol as the solvent impregnating the packing material. The tests were performed at normal stresses of 250 kPa, 500 kPa, 1,000 kPa, and 3,000 kPa, and several replicate determinations were made at most normal stresses. Figure 12 illustrates the shear stress deformation observed as a response to the shear stress applied. The resulting Mohr–Coulomb failure envelope is also shown in Figure 11. The test results suggest that the contact between the silica sample and the stainless steel plate followed a Mohr–Coulomb failure law with a cohesion $C = 0$ kPa, and a friction angle $\delta = 22.5°$ (tan $\delta =$ 0.415).

Zorbax consolidated from a slurry in acetone tends to have a slightly higher friction angle (difference, $\Delta\delta = 1.36°$) than when this material is consolidated from methanol. However, this difference is nearly insignificant, which is consistent with the commonly accepted theories of contact friction. This small difference suggests that the wall friction in the HPLC columns is independent of the nature of the solvent. If not entirely insignificant, the small difference might be due to the fact that particles interact strongly with each other in the packed bed and that this interaction depends on the surface tension between the liquid and the solid, tension which differs markedly from solvent to solvent. As a result, the radial stress applied by the bed against the wall would depend on the nature of the solvent. This is the only reasonable explanation to the apparent contradiction between a friction coefficient practically independent of the nature of the solvent (Figure 11) and a shear strength at the interface between the wall of a chromatographic column and a bed of Zorbax C18 prepared from slurries of the material in different solvents which depends on the nature of the solvent (Guiochon et al., 1999). This aspect of the problem warrants further investigation.

(b) Results from Kromasil. Shear tests were also conducted with Kromasil C8, following the same procedure as described earlier (Experimental). These tests were carried out under normal stresses of 1,000, 2,000 and 3,000 kPa, with the packing material being consolidated from a methanol slurry. These experiments were repeated several times. The plot of the shear stress vs. the horizontal displacement of the shear box (Figure 6) are shown in Figure 13. The resulting Mohr–Coulomb failure envelope is shown in Figure 11. The best estimate of the coefficients of Eq. 11 give $C = 0.0$ kPa and $\delta = 11.6°$ (tan $\delta = 0.206$). This is an important result, because it demonstrates a rather large difference between two packing materials. The friction coefficient of Kromasil C8 is

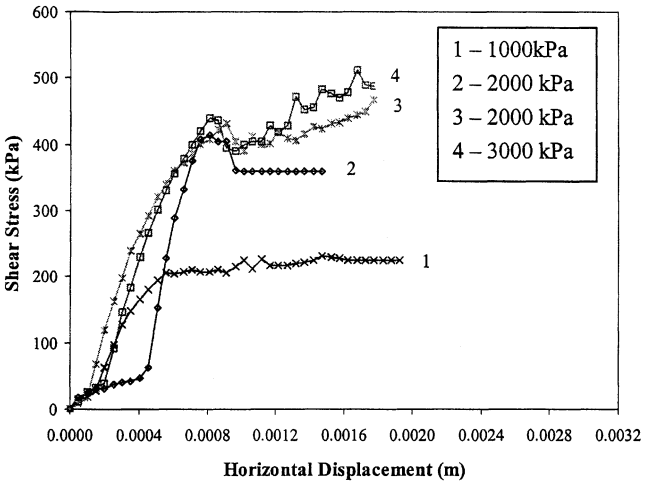

Figure 13. Shear stress vs. horizontal displacement for Kromasil consolidated from a slurry in methanol.

nearly half that of Zorbax C18. The difference may be explained by a difference in the morphology of the particles (see Figures 7a and 7b), through either their interaction with the steel surface or through their mutual interactions with the other particles in the bed. The Kromasil particles are nearly perfect spheres, while the Zorbax particles are not (Sarker et al., 1996).

(c) Shear Strength of Interface and Angle of Internal Friction. There is a relationship between the angles of internal friction (that is, between particles) and of friction at the wall (Potyondy, 1961) and this relationship seems verified for both materials. The interface friction angle for the contact between an assembly of particles and a surface δ is often expressed as a fraction of the internal friction angle ϕ of the material itself (Potyondy, 1961). Typical soils and construction materials are observed to have interface friction angles δ ranging from about 0.5 to 1 times ϕ. Thus, based on the values of ϕ for the bulk packing material (Mihlbachler et al., 1998), and the measured values of δ reported above, an interface ratio of $\delta/\phi = 21/36 = 0.58$ is obtained for the Zorbax-steel interface, while δ/ϕ of $11.6/23 = 0.50$ is obtained for the Kromasil-steel interface. These values are consistent with the values suggested by Potyondy (1961) for smooth interfaces. This comparison assumes, however, that the friction coefficient is the same for C18-bonded and for unbonded silica particles.

The comparison of the results of two different friction experiments performed both with these two materials, Zorbax and Kromasil, reveals an intriguing apparent contradiction. As just shown, the friction coefficient of Kromasil against a stainless steel wall (0.20) is approximately twice smaller than that of Zorbax (0.41). By contrast, the stress required to expel a 5 cm ID packed, consolidated bed from a stainless steel chromatographic column is slightly more than three times larger when the bed is packed with Kromasil than when it is packed with Zorbax (Cherrak et al., 2001). A possible explanation for this opposite behavior in two different types of friction experiments is that the radial stress applied by the bed to the wall is much larger in the case of Kromasil than in the case of Zorbax. A similar reason could explain the influence of the nature of the solvent on the stress required to expel the bed from the column (Cherrak et al., 2001). In both cases, it is speculated that the nature of the solvent may affect the manner in which the particles interact and compact, which will have a direct relationship on the ratio of the radial to axial stress. This relationship between the radial and axial stresses in an elastic material is the same as the relationship between the radial and axial strains, which is known as Poisson's ratio (Lambe and Whitman, 1979; Holtz and Kovacs, 1981; Bardet, 1997). In both cases, whether the packing solvent or the packing material is changed, the range of radial stress experienced seems to be barely short of one order of magnitude, a considerable effect. Poisson's ratio seems to have a large importance on the behavior of packing materials. Unfortunately, this parameter is most difficult to measure and a value must be assigned to it based on conventional correlations (Yew et al., 2003). Further investigation into the relationship between the properties of the pore fluid and the mechanical properties and stress state in the packing material is under way.

Influence of lubricant on the friction coefficient of bed

Wall friction is thought to contribute to the nonhomogeneity of a bed of packing material. This is confirmed by the results of modeling of the bed behavior during its consolidation (Yew et al., 1999). Thus, an experimental investigation of the influence of several potential wall lubricants was conducted in an attempt to further reduce the friction coefficient at the interface. Prior to conducting direct shear tests with the lubricants, the relative importance of the influence of different potential lubricants was investigated using the tilt test (see Experimental Procedures section). The lubricant with the best potential for reducing the wall friction was selected to conduct shear tests with the lubricated stainless steel plate and the Zorbax material.

(a) Results of the Tilt Test. Since friction at the interface between the packing material and the stainless steel column leads directly or indirectly to a decrease in the efficiency of chromatographic columns, several wall lubricants were investigated. The tilt tests were chosen to operate this selection because they are easy, inexpensive, and rapid to operate and allow the easy selection of the best lubricants for further studies.

The coefficient of friction ($\tan \delta$) obtained in these tests is compared in Figure 14. For reference, the coefficient of friction for the phenolic block without lubricant is also shown. This unlubricated value of 0.24 compares favorably with that of Zorbax ($\tan \delta = 0.387$) and Kromasil ($\tan \delta = 0.212$) with methanol, which were measured in the direct shear tests. Sprayon flake graphite spray (density, 0.66 g/cm^3) was identified as the lubricant with the best potential for reducing the friction between the bed and the column wall (Figure 14). A series of direct shear tests were then conducted between the stainless steel plate lubricated with Sprayon graphite spray and the Zorbax material to observe the possible effects of the lubricant on the interface friction between the plate and the packing materials.

(b) Direct Shear Tests with Lubricant. The same method described earlier (Experimental) was used, except that

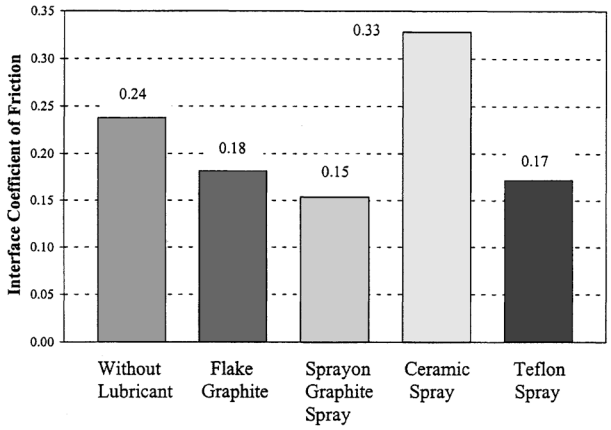

Figure 14. Interface coefficient of friction between a block of phenolic resin and the steel plate lubricated with various products.

Sprayon graphite was now used as a coating on the stainless steel plate. The shear stress displacement response is shown in Figure 15. The resulting Mohr–Coulomb failure envelope (Figure 11) was obtained based on the peak failure shear stresses. The test results suggest that the contact between the silica sample and the lubricated stainless steel plate followed a Mohr–Coulomb failure law with a cohesion $C = 0$ kPa, and a friction angle $\delta = 18.3°$ (tan $\delta = 0.33$). In other words, the graphite spray reduced the coefficient of friction by about 15%. This reduction is less important than that observed in the tilt tests (37.5%). This might be explained in part by the difficulty of achieving and maintaining a uniform coating of the steel plate under the packing material. It has to do with the chemical difference between the surfaces of the phenolic resin block and the agglomerate of silica particles.

Finally, the shear test results are summarized in Figure 11, which compares the Mohr–Coulomb failure envelopes for the interfaces with the two packing materials (Zorbax and Kromasil) studied, with two different solvents (methanol and acetone), and with or without lubrication of the interface. As illustrated in this figure, the lowest interface coefficient of friction between the silica sample and the stainless steel plate is found for the combination of Kromasil C8 and methanol (tan $\delta = 0.21$). This suggests that a more homogeneous column could be prepared with Kromasil than with Zorbax. In contrast, the largest coefficient of friction (tan $\delta = 0.39$) was obtained with the combination of Zorbax and acetone.

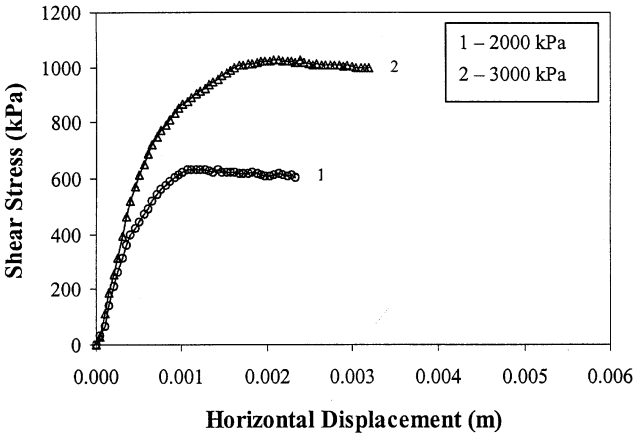

Figure 15. Shear stress vs. horizontal displacement for Zorbax consolidated from a slurry in methanol and a steel plate lubricated with graphite.

Conclusions

In order to model the mechanical and hydraulic behavior of silica packing materials during the preparation of chromatography columns, a series of laboratory tests based on those commonly employed in soil mechanics were conducted. The permeability of beds of packing materials with methanol as the liquid phase was measured, and the mechanical properties of the contact between the packing material and the stainless steel column walls evaluated for various combinations of packing materials and solvents. The reduction in the interface coefficient of friction due to the introduction of lubricants was also investigated.

The results obtained are disappointing regarding the reduction in the interface friction angle by the lubrication of the steel plate. It is doubtful that such a slight reduction in the friction angle could justify the introduction in the column of a material, graphite, which could affect the retention properties and, potentially, cause some tailing due to being concentrated at the column wall. Admittedly, only a minute amount would be required: a 3.5 μm thick layer coated on the wall of a 5 cm ID, 20 cm long column represents a volume of 0.11 mL of graphite in a 393 mL column, or 0.03% of the column volume. This graphite does not need to have a high specific surface area.

The testing of packing materials for chromatography, the determination of the mechanical properties of these materials, and the description of the stress conditions at the contact between the packing material and steel contact provide new insights into the mechanisms governing the preparation of chromatography columns. As we will show in Part II of this article (Yew et al., 2003), knowing the material properties determined in the laboratory tests described here permits the numerical modeling of the column preparation process. The results of an accurate modeling of the rheologic behavior of the packing material during consolidation of the slurry into a bed, at least for the two materials discussed in this work, suggest more promising approaches to improve the column efficiency than the introduction of lubricants.

Acknowledgments

This work was supported in part by Grant DE-FG05-88-ER13869 of the U.S. Department of Energy and by the cooperative agreement between the University of Tennessee and the Oak Ridge National Laboratory. We acknowledge the loan of the LC.50.VE.500.100 column skid by PROCHROM (Champigneulles, France), the generous gift of the Kromasil packing material used in this work by Lars Torstensson (Eka Nobel), and that of the Zorbax packing material by Klaus Lohse (BTR Separations).

Notation

a = cross-sectional area of the graduated burette (permeability measurement)
a_v = compressibility of the bed
A = cross-sectional area of a sample of packing material

C = cohesion or cohesive strength of the material contact
C_C = compression index
C_s = swelling index
C_v = coefficient of consolidation
d_{10} = particle size such that smaller particles account for 10% of the weight
d_{90} = particle size such that smaller particles account for 90% of the weight
$d_{\max}$ = maximum particle diameter of the packing material
$d_{\min}$ = minimum particle diameter of the packing material
D = sample diameter
e, e_I = void ratio of the packing material, void ratio at point I
e_0 = initial void ratio
f = coefficient of pore shape used in the Kozeny–Carman equation
F = phase ratio in liquid chromatography
g = gravitational acceleration
G_s = specific gravity of the packing material
h = head pressure of a liquid (or ΔP)
h_f = elevation of methanol solvent in the standpipe above the discharge level at time t
h_i = elevation of methanol solvent in the standpipe above the discharge level at time $t = 0$
h_0 = initial sample height
h_t = sample height at time t
H_0 = initial height of the sample in the shear box
H_1 = vertical distance measured with a caliper
H_2 = depth of the shear box
H_3 = height of the top cap on the shear box
H_4 = thickness of the filter paper in the shear box
$\Delta h = h_0 - h_t$
k = permeability coefficient or hydraulic conductivity
K = intrinsic permeability or permeability (Eqs. 6 and 7)
L = length of the sample of packing material (such as column bed)
M_s = mass of the dry sample
p = mechanical stress
ΔP = inlet or hydraulic head pressure
R = resisting force against sliding
S = specific surface area exposed to viscous shear (that is, of the outside boundary of the particles)
t = time
T = shear force (also pseudo time constant in Terzaghi theory, Eq. 1)
u = cross-section average velocity of the liquid percolating through a bed
V = volume of the sample at time t
V_1 = initial volume of the sample
V_e = external pores volume
V_i = internal pores volume $V_i = V_o - V_e$
V_o = total volume occupied by the solvent
$V_{\text{particles}}$ = volume of the silica particles, consists of the volume inaccessible to the solvent (V_u) and the internal pores volume (V_i) $V_{\text{particles}} = V_T - V_e$
V_s = total volume of the silica particles
V_T = total column volume $V_T = V_e + V_i + V_u$
V_u = volume inaccessible to the solvent $V_u = V_T - V_o$
W = weight of the phenolic block in the tilt test

Greek letters

α = angle of the plane surface and the horizon in the tilt test
γ_w = specific weight of the liquid
δ = interface friction angle
ϵ_e = external porosity
ϵ_i = internal porosity
ϵ_T = total porosity
ϵ_v = volumetric strain
ϵ_z = axial strain
η = kinematic viscosity of the liquid
σ = total or axially applied stress (normal stress)
σ_{11}, σ_{22}, σ_{33} = principle stresses
σ_y = normal stress
σ' = effective stress
σ'_P = pre-consolidation stress
μ = dynamic viscosity of the liquid
ρ_{d0} = initial density of the dry sample
ρ_{dry} = apparent density of the dry packed bed
$\rho_{\text{particles}}$ = density of the silica particles
ρ_u = density of solid silica
ρ_w, ρ = density of the liquid
τ, τ_{xy} = shear stress
ϕ = internal friction angle
ϕ_p = peak friction angle
ϕ_r = residual friction angle

Literature Cited

Bansal, N. P., and N. R. H. Doremus, *Handbook of Glass Properties*, Academic Press, New York (1986).

Bardet, J.-P., *Experimental Soil Mechanics*, Prentice Hall, Upper Saddle River, NJ (1997).

Baur, J. E., E. W. Kristensen, and P. M. Wightman, "Radial Dispersion from Commercial High-Performance Liquid Chromatography Columns Investigated with Microvoltammetric Electrodes," *Anal. Chem.*, **60**, 2334 (1988).

Baur, J. E., and R. M. Wightman, "Microcylinder Electrodes as Sensitive Detectors for High-Efficiency, High-Speed Liquid Chromatography," *J. Chromatog.*, **482**, 65 (1989).

Bayer, E., E. Baumeister, U. Tallarek, K. Albert, and G. Guiochon, "NMR Imaging of the Chromatographic Process. Deposition and Removal of Gadolinium Ions on a Reversed-Phase Liquid Chromatographic Columns," *J. Chromatog. A*, **704**, 37 (1995).

Bayer, E., W. Müller, M. Ilg, and K. Albert, "Visualization of Chromatographic Separations by NMR Imaging," *Angew. Chem. Int. Ed.*, **28**, 1029 (1989).

Bird, R. B., W. E. Stewart, and E. N. Lightfoot, *Transport Phenomena*, Wiley, New York (1960).

Broyles, B. S., A. Shalliker and G. Guiochon, "Calculation of Axial and Radial Diffusion Coefficients in a Liquid Chromatography Column," *J. Chromatog.*, in press (2002).

Cherrak, D., M. Al-Bokari, E. C. Drumm, and G. Guiochon, "Packing Behavior of Luna C18 in Axially Compressed Chromatographic Columns," *J. Chromatog. A*, **943**, 15 (2001).

Desai, C. S., and J. F. Abel, *Introduction to the Finite Element Method*, Van Nostrand–Reinhold, New York (1972).

Eon, C. H., "Comparison of Broadening Patterns in Regular and Radially Compressed Large-Diameter Columns," *J. Chromatog.*, **149**, 29 (1978).

Farkas, T., J. Q. Chambers, and G. Guiochon, "Column Efficiency and Radial Homogeneity in Liquid Chromatography," *J. Chromatog.*, **679**, 231 (1994).

Farkas, T., M. J. Sepaniak, and G. Guiochon, "Column Radial Homogeneity in HPLC," *J. Chromatog.*, **740**, 169 (1996).

Farkas, T., M. J. Sepaniak, and G. Guiochon, "Radial Distribution of the Flow Velocity, The Column Efficiency, and the Concentration Profile at the Outlet of a Preparative Scale HPLC Column," *AIChE J.*, **43**, 1964 (1997).

Farkas, T., and G. Guiochon, "Contribution of the Radial Distribution of the Flow Velocity to Band Broadening in HPLC Columns," *Anal. Chem.*, **69**, 4592 (1997).

Freeze, R. A., and J. A. Cherry, *Groundwater*, Prentice Hall, Englewood Cliffs, NJ (1979).

Giddings, J. C., and E. N. Fuller, "Particle Size Nonuniformity in Large Scale Columns," *J. Chromatog.*, **7**, 255 (1962).

Guiochon, G., S. G. Shirazi, and A. M. Katti, *Fundamentals of Preparative and Nonlinear Chromatography*, Academic Press, Boston (1994).

Guiochon, G., and M. Sarker, "Consolidation of the Packing Material in Chromatographic Columns under Dynamic Axial Compression: I. Fundamental Study," *J. Chromatog. A*, **704**, 247 (1995).

Guiochon, G., T. Farkas, H. Guan-Sajonz, J. Koh, M. Sarker, B. Stanley, and T. Yun, "The Consolidation of Particles and the Packing of Chromatographic Columns," *J. Chromatog. A*, **762**, 83 (1997).

Guiochon, G., E. C. Drumm, and D. Cherrak, "Evidence of a Wall Friction Effect in the Consolidation of Beds of Packing Materials in Chromatographic Columns," *J. Chromatog. A*, **835**, 41 (1999).

Holtz, R. D., and W. D. Kovacs, *An Introduction to Geotechnical Engineering*, Prentice Hall, Englewood Cliffs, NJ (1981).
Horne, D. S., J. H. Knox, and L. McLaren, "A Comparison of Mobile Phase Peak Dispersion in Gas and Liquid Chromatography," *Sep. Sci. Technol.*, **1**, 531 (1966).
Jaeger, H. M., S. R. Nagel, and R. P. Behringer, "Granular Solids, Liquids, and Gases," *Rev. Modern Phys.*, **68** 1259 (1996).
Jenike, A. W., "Storage and Flow of Solids," *Bulletin No. 123*, University of Utah, Utah Engineering station, **23**(26), 1 (Nov. 1964).
Jumikis, A. R., *Theoretical Soil Mechanics*, van Nostrand, New York (1969).
Knox, J. H., G. R. Laird, and P. A. Raven, "Interaction of Radial and Axial Dispersion in Liquid Chromatography in Relation to the 'Infinite Diameter Effect'," *J. Chromatog.*, **122**, 129 (1976).
Lambe, T. W., and R. V. Whitman, *Soil Mechanics. SI Version*, Wiley, New York (1979).
Lightfoot, E. N., "The Invention and Development of Process Chromatography: Interaction of Mass Transfer and Fluid Mechanics," *Amer. Lab.*, **31**, 13 (1999).
Loudon, A. G., "The Computation of Permeability from Simple Soil Tests," *Geotechnique*, **28**, 165 (1952).
Martin, M., G. Blu, and G. Guiochon, "The Effect of Pressure on the Retention Time and the Retention Volume of an Inert Compound in Liquid Chromatography," *J. Chromatog. Sci.*, **11**, 641 (1973).
Mihlbachler, K., T. Kollmann, A. Seidel-Morgenstern, J. Tomas, and G. Guiochon, "Measurement of the Degree of Cohesion of Two Native Silica Packing Materials," *J. Chromatog. A*, **818**, 155 (1998).
Potyondy, J. G., "Skin Friction between Various Soils and Construction Materials," *Geotechnique*, **11**, 339 (1961).
Sarker, M., A. M. Katti, and G. Guiochon, "Consolidation of the Packing Material in Chromatographic Columns under Dynamic Axial Compression: II. Consolidation and Breakage of Several Packing Materials," *J. Chromatog. A*, **719**, 275 (1996).
Schwedes, J., and D. Schultze, "Measurement of Flow Properties of Bulk Solids," *Powder Technol.*, **61**, 59 (1990).
Sofer, G. K., and L. E. Nyström, *Process Chromatography. A Practical Guide*, Academic Press, London (1989).
Stanley, B. J., M. Sarker, and G. Guiochon, "Consolidation of the Packing Material in Chromatographic Columns under Dynamic Axial Compression: IV. Mechanical Properties of some Packing Materials," *J. Chromatog. A*, **741**, 175 (1996).
Tallarek, U., E. Baumeister, K. Albert, E. Bayer, and G. Guiochon, "NMR Imaging of the Chromatographic Process. Migration and Separation of Bands of Gadolinium Chelates," *J. Chromatog. A*, **696**, 1 (1995).
Tallarek, U., K. Albert, E. Bayer, and G. Guiochon, "Measurement of Transverse and Axial Apparent Dispersion Coefficients in Packed Beds," *AIChE J.*, **42**, 3041 (1996).
Taylor, D. W., *Fundamentals of Soil Mechanics*, Wiley, New York (1948).
Terzaghi, K., *Erdbaumechanik auf Bodenphysikalischer Grundlage*, Section 20, Deuticke, Leipzig, Germany (1925).
Tomas, J., "Modeling Time Consolidation Processes of Bulk Materials—Problems and Preliminary Solutions," *Proc. Int. Symp. on Reliable Flow of Particulate Solids*, G. C. Enstad, ed., Porsgrunn, Oslo, Norway, 342 (1993).
Tomas, J., *Zum Verfestigungsprozess von Schuettguetern*, Mikroprocesse und Kinetikmodelle, Chemie Ingenieur Technik, 69 4, p. 455 (1997).
Train, D., "An Investigation into the Compaction of Powders," *J. Pharm. Pharmac.*, **8**, 745 (1956).
Train, D., "Transmission of Forces through a Powder Mass during the Process of Pelleting," *Trans. Instn. Chem. Engrs.*, **35**, 258 (1957).
Visser, A. D., *Elsevier's Dictionary of Soil Mechanics* (in four languages), Elsevier, Amsterdam, The Netherlands (1965).
Yew, G. G., "Application of Soil Mechanics and the Finite Element Method to High Performance Liquid Chromatography Columns," Master's Degree Diss., The University of Tennessee, Knoxville, TN (1999).
Yew, B. G., E. C. Drumm, and G. Guiochon, "Simulation of Wall Friction Effects in High Performance Liquid Chromatography (HPLC) Columns," *Proc. of Fourth Int. Conf. on Constitutive Laws for Eng. Mat.*, Rensselaer Polytechnic Institute, Troy, NY (1999).
Yew, B. G., J. Ureta, R. A. Shalliker, E. C. Drumm, and G. Guiochon, "Mechanics of Column Beds: II. Modeling of Coupled Stress-Strain-Flow Behavior," *AIChE J.*, **49**, 642 (2003).
Zienkieweicz, O. C., *The Finite Element Method in Engineering Science*, McGraw-Hill, London (1971).

Manuscript received Oct. 26, 2001, and revision received Aug. 27, 2002.